

Improving the Performance of UV-Curable Coatings with Carbon Nanomaterials

Yun JIANG¹, Andy ZHANG^{2,3}, Steven YU³, Nick YIN³, Willy DU³, Tao ZHANG^{1,*}

1. College of Engineering and Applied Sciences, Nanjing University, Nanjing 210093, China

2. Department of Macromolecular Science, Fudan University, Shanghai 200433, China

3. Guangzhou Wraio Chemicals Co., Ltd., Guangzhou 510653, China

Abstract: By combining a trifunctional urethane acrylate synthesized from a hexamethylene diisocyanate trimer and caprolactone acrylate with a bifunctional urethane acrylate prepared from hydroxyethyl acrylate and isophorone diisocyanate, a new reactive resin was prepared, and trimethylolpropane triacrylate was chosen as the thinner to constitute a novel coating matrix. Different amounts of multi-functionalized carbon nanotubes (CNTs) and graphene oxide (GO) were introduced into the matrix and cured by ultraviolet radiation, producing the UV-cured coatings. Utilizing the methods of Fourier transform infrared spectroscopy, UV-vis spectroscopy, wide angle X-ray diffraction and thermogravimetric analysis, the chemical structures and physical properties of the coatings were analyzed. A series of ASTM methods, such as pencil hardness classification, RCA abrasion, crosscut adhesion test classification, and chemical resistance rub testing, were applied to investigate the performances of the coatings. It was found that the introducing a small amount of carbon nanomaterials can improve the thermal stability, surface hardness, adhesion, abrasive resistance, and chemical resistance performance of the UV-curable coatings. The reasons and mechanisms of the performance improvements are discussed in this work.

Keywords: polyurethane acrylate, UV-curable coating, carbon nanotube, graphene oxide

1. Introduction

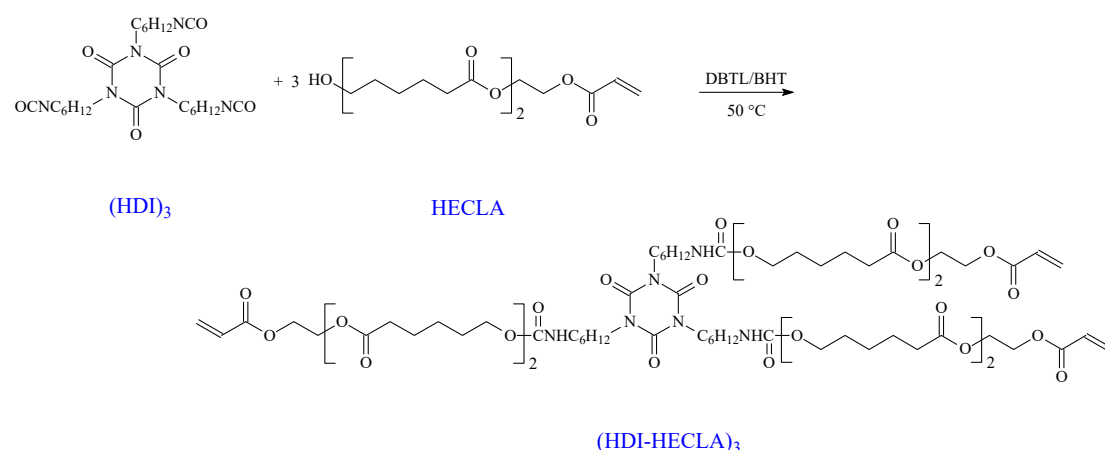
The performances of the UV-curable coatings, such as the surface hardness, adhesion to substrate, chemical resistance property, gloss and abrasive resistance, are determined by the formulation of the coating system. The requirements for the ingenious formulation designs and performance improvements in UV-curable coatings are growing continuously, along with the expansion of their potential applications. In 2015, 467.9 kilo-tons of reactive resins were produced worldwide, with a value of 2.21 billion US dollars. By 2024, the output will reach 1000 kilo-tons, with a value of 4.67 billion US dollars [1].

In this study, a trifunctional urethane acrylate composed of a hexamethylene diisocyanate trimer ((HDI)₃) and caprolactone acrylate (HECLA) coordinated with a

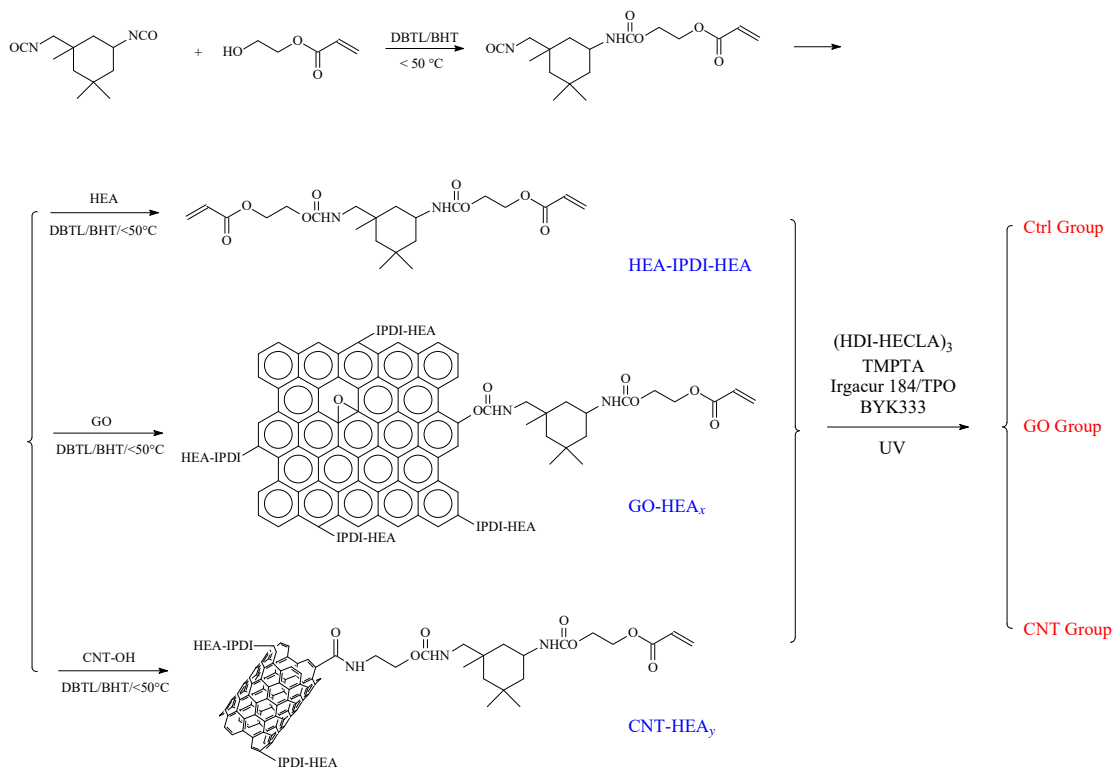
bifunctional urethane acrylate synthesized from hydroxyethyl acrylate (HEA) and isophorone diisocyanate (IPDI) was used as the reactive resin. Trimethylolpropane triacrylate (TMPTA) was chosen as a thinner to constitute a novel matrix of UV-curable coatings. The carbon nanomaterials, carbon nanotubes (CNTs) and graphene oxide (GO), were functionalized by an acrylate reaction with IPDI and HEA and were introduced into the matrix at various quantities. The chemical structures, physical properties and performances of the obtained coating were characterized, analyzed and investigated. The coating performance was a focus, and the effects of the type and amount of carbon nanomaterials are discussed. It is desirable to provide performance improvements by introducing nanomaterials into the organic coating, include the surface hardness, adhesion, abrasive resistance, chemical resistance, etc.

2. Experiments

The tri-functional polyurethane acrylate (HDI-HECLA)₃ was synthesized as Scheme 1 and used as the main matrix of the UV-curable coating. To homogeneously disperse the nanomaterials into the UV-curable coating system, modified GO and CNTs were reacted with the acrylate system according to Scheme 2. Based on Table 1, various amounts of trifunctional (HDI-HECLA)₃ acrylate resin, HEA-IPDI-HEA bifunctional acrylate resin, 2% GO-HEAx in DMF or 2% CNT-HEAy in DMF, photoinitiator Irgacure 184 and Irgacure TPO, reactive diluents TMPTA and leveling agent BYK-333 were mixed with a high-speed mixer, followed by adding a suitable amount of DMF to regulate the viscosity of the mixtures. The mixtures were then sprayed onto polycarbonate (PC) sheets, dried at 60 °C for 5 minutes, and cured under a UV lamp with an exposure energy of 800 mJ/cm². The final coatings on the PC sheets were approximately 20 μm thick and stored at room temperature for further studies.



Scheme 1. Synthesis of trifunctional polyurethane acrylate



Scheme 2. Synthesis and preparation route of modified carbon nanomaterials and coating samples

Table 1. Mixture formulations for spray coatings

Sample code ^a	Actual content of GO or CNTs in the coating samples (%) in Mass	(HDI-HECLA) ₃ (g)	HEA-IPDI-HEA (g)	2% GO-HEA _x in DMF (g)	2% CNT-HEA _y in DMF (g)
0.2Ctrl	/	90	10	/	/
0.4Ctrl	/	80	20	/	/
0.6Ctrl	/	70	30	/	/
0.8Ctrl	/	60	40	/	/
1.0Ctrl	/	50	50	/	/
0.2GO	0.168	90	/	10	/
0.4GO	0.351	80	/	20	/
0.6GO	0.552	70	/	30	/
0.8GO	0.774	60	/	40	/
1.0GO	1.019	50	/	50	/
0.2CNT	0.168	90	/	/	10
0.4CNT	0.351	80	/	/	20
0.6CNT	0.552	70	/	/	30
0.8CNT	0.774	60	/	/	40
1.0CNT	1.019	50	/	/	50

a. in every sample, 20 g of TMPTA, 2 g of Irgacure 184, 2 g of Irgacure TPO and 0.4 g of BYK-333 were also included.

The Fourier transform infrared (FTIR), UV-vis spectra, wide angle X-ray diffraction (WAXD), thermogravimetric analysis (TGA) were performed to characterize the structures and the properties of coating samples. The pencil hardness of the UV-cured coating was determined using ASTM D3363-05. The crosscut adhesion tests were performed according to ASTM D3359-08, and the RCA abrasion tests were carried out following ASTM F2357-10 with force of 175 g. The gloss measurements were performed at 60.2° according to ASTM D523-14. The solvent (ethanol and butanone) resistance of the coatings was investigated using solvent rubs (ASTM D5402-15) with an alcohol abrasion tester. The boiling resistance tests were carried out according to ASTM D879.

3. Results and Discussion

3.1. Chemical structure, appearance and physical properties investigation

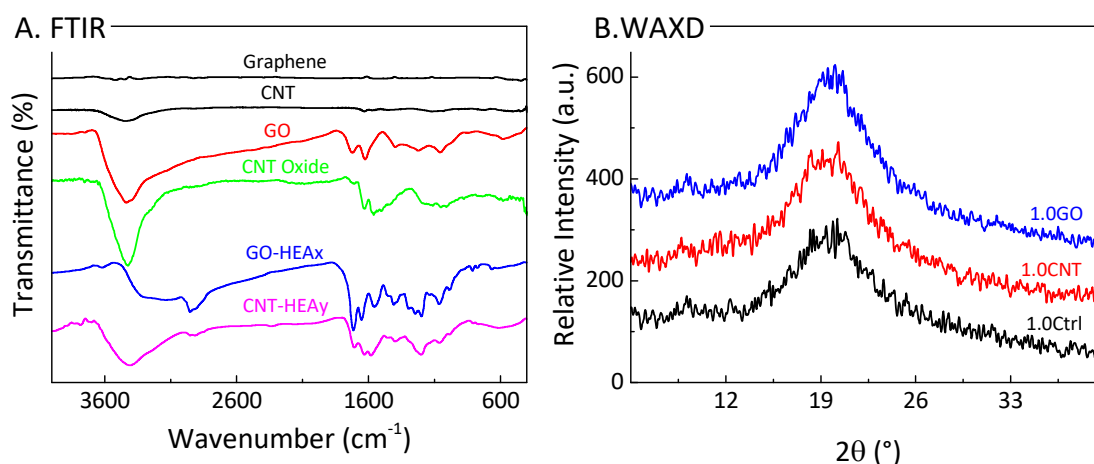


Figure 1. FTIR spectrum of raw, intermediate and final modified carbon nanomaterials (A) and WAXD curves (B) for typical coating films.

To confirm the chemical modifications from the carbon nanomaterials, the crude GO and CNTs products that reacted with IPDI and HEA were thoroughly washed with ethanol. The obtained solid products, GO-HEAx and CNT-HEAy were vacuum dried at room temperature and scanned with FTIR along with the raw carbon nanomaterials and intermediate products, as shown in Figure 1A. The obvious spectrum changes of the FTIR from the raw carbon nanomaterials in the final products proved the successful modification on the pristine graphene and nanotubes. WAXD was used to investigate the crystallization of films, as shown in Figure 1B. From the curves, it was found that even when the incorporated carbon nanomaterials were at a weight percent as high as 1.0%, the WAXD pattern did not present an obvious change. The UV-cured coatings exhibit a semi-crystal state.

Figure 2 presents the quantitative UV-Visible spectra of the coating film with 1.0% carbon nanomaterials and the images of the UV-cured coatings. The control coating films without carbon materials were transparent, but the samples with carbon

nanomaterials showed an increasing chromaticity with increasing amounts of CNTs and GO. For the CNT samples, the coating showed an increasing grayscale, and the color become darker. For GO, the coatings became brown, and the color also grew deeper. In the visible range from 400 to 600 nm, the coatings without carbon nanomaterials are nearly colorless and have a transmittance higher than 90%. For the coating films containing 1.0% CNT, the transmittance is approximately 50 – 60%. For the GO group, the color is deeper than that of both the Ctrl group and CNT group, with a transmittance that decreases to 30 – 50%. The higher absorbance in the 300 – 500 nm range leads to a brown appearance of the coating films. The darker chromaticity of the coating containing carbon nanomaterials is not suitable for situations where colorlessness and transparency are important. However, for color coatings, the incorporation of carbon nanomaterials can potentially be applied.

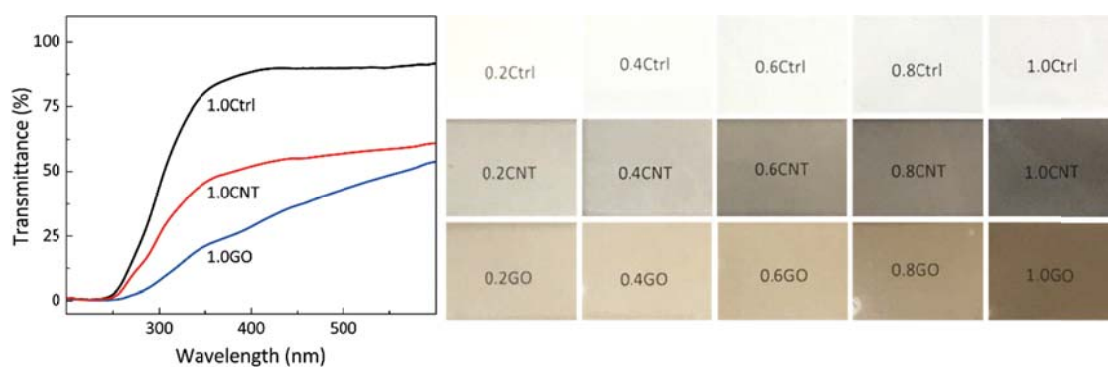


Figure 2. UV-visible spectra for typical coating films and images of UV-cured coatings with and without carbon nanomaterials

Figure 3 shows the thermogravimetry curves of the UV-coating film samples. As shown in Figure 3, the degradation process and thermal stability were dependent on the chemical structures of the samples. The degradation process of the coating films could be divided into 3 steps. The thermal degradation of the polyurethane acrylate films with bifunctional HEA-IPDI-HEA occurred in the temperature range of 160 – 280 °C for the first step, at 280 – 400 °C for the second step, and at 400 – 450 °C for the third step. The low degradation temperature, especially for the HEA-IPDI-HEA, was mainly attributed to fewer stable urethane groups existing in the aliphatic polyurethane acrylates, which could decompose to form alcohol and isocyanate groups. The results obtained here agree with the literature [2, 3]. Additionally, with the introduction of additional multi-functional modified CNT and GO, more bifunctional HEA-IPDI-HEA was injected, which led to a decrease in the thermal stability. In Figure 4D, the onset main decomposition temperature of the Ctrl group decreased by approximately 20 °C when changing from a 10% to 50% mass ratio of bifunctional HEA-IPDI-HEA. This trend was also investigated in the CNT and GO groups. However, the addition of multi-functional modified CNTs and GO reversed the trend to a certain degree. For every addition, the coating film containing CNTs and GO presented a higher onset decomposition temperature than did the corresponding coating film without CNTs and GO. Comparing the onset decomposition temperatures of the CNT and GO group, for every addition, no

significant differences were found. This result indicates that the introduction of CNTs and GO can improve the thermal stability of the polyurethane acrylate UV-curable coating system.

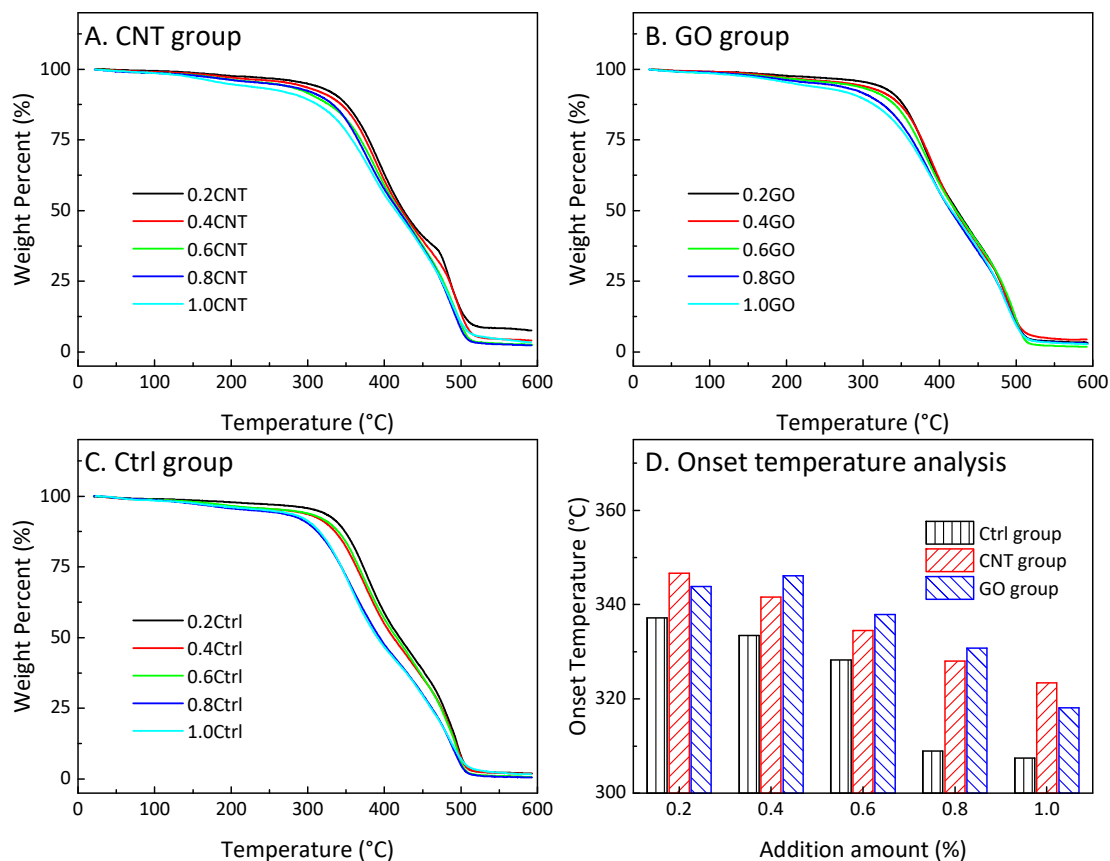


Figure 3. Thermogravimetry analysis of UV-cured coatings of the (A) CNT group, (B) GO group, and (C) Ctrl group and the (D) onset temperature analysis results

In general, the thermal degradation of the polyurethane acrylate is associated with changes in the C=O and C-N urethane groups. Additionally, some urea compounds may be formed during the thermal degradation of polyurethane acrylate at a high temperature. The enhancement of the thermal stability can be attributed to the higher overall crosslinking density caused by the multi-functional modified CNTs and GO. The crosslinking density of the UV-cured films increased with the increasing functionality of the modified carbon nanomaterials, which may have induced the higher thermal stability in the coating films with multi-functional CNT-HEAx and GO-HEAy. Moreover, the thermal stability of the CNT and GO themselves was much higher than that of the polyurethane acrylate, which could also have improved the thermal stability of the coating films, even with a concentration as low as 0.2% in mass.

3.2. Coating performance testing by ASTM methods

As a kind of UV-curable coating, various typical performances were investigated in non-controversial ways according to the ASTM standard, as summarized in Table 2.

The pencil hardness class depends mainly on the chain flexibility of the molecule and crosslinking density of the coating [4]. Specifically, the improved flexible structure of the oligomer leads to a reduction in the hardness of the film, but the improved crosslinking density of the coating film causes the opposite effect. In general, a curing film with good flexibility and a low crosslinking density produces a poor pencil hardness, but the properties of good hardness would be obtained with a poor flexibility and high crosslinking density. In our system, the content of the double bond of the system determines the crosslinking density, and the HECLA moiety dictates the flexible structure of the film. The structure of the CNT and GO group coating films were composed mainly of trifunctional (HEA-CELA)₃ and bifunctional HEA-IPDI-HEA, with small amounts of multi-functional carbon nanomaterials. In the Ctrl group, with an increase in the amount of bifunctional HEA-IPDI-HEA, the crosslinking density was decreased, but the flexible CELA moieties were replaced by short and rigid HEA-IPDI-HEA segments. Thus, the pencil hardness class increased from 1B to HB. By introducing multi-functional modified nanomaterials, the crosslinking density increased further, leading to the further improvement of the hardness. The pencil hardness class was found to begin from HB and ultimately reached F. Between the CNT and GO groups, there was no significant difference in the pencil hardness found, which indicates that the fibroid CNT and sheet GO can both improve the hardness performance of the coating film.

The crosscut adhesion class expressed the adhesive performance of the UV-cured coating. The resulting 5B class represented the highest class of adhesion, which means that no area was removed by the tape and no flaking occurred. These results indicate that all the samples in our system presented excellent adhesive performance on the PC substrate and that the limited increase (from 1B to F) of the surface hardness did not lead to the complete hardening of the coating film, which often leads to a decrease in the adhesive performance.

The abrasive test is an accurate and repeatable way to determine the abrasion wear characteristics of inks and coatings [3]. The RCA abrasion test presents the combined properties of surface hardness, rigidity and adhesion of the surface coating and are typically used in the 3C (Computer, Communication and Consumer Electronics) industry to test the surface for resistance to abrasion and wear. In general, the RCA abrasion in every group shows improvement with an increasing amount of rigid HEA-IPDI-HEA segments. In the Ctrl group, the highest increase reached 40%. Comparing the samples in different groups, the RCA abrasion was markedly increased when the modified multi-functional carbon nanomaterials were introduced, which can be attributed to the increased crosslinking density and, equally importantly, to the rigidity of the carbon nanomaterials themselves. In addition, the CNTs and GO show no significant difference in improving the RCA abrasion of our system. However, when the carbon nanomaterials were introduced with as much as 1.0% in mass, the RCA abrasion of the CNT and GO groups decreased dramatically, to the same level expressed by the corresponding sample in the Ctrl group. These phenomena are attributed to the phase separation caused by the aggregation of the nanomaterials.

When the amounts of nanomaterials exceeded 1%, the interface energy accompanied by the huge surface area of the nanomaterials made it difficult to homogeneously distribute and separate in liquid organic coatings. This led to an obvious aggregation during curing and phase separation in the resulting film, thus decreasing the RCA abrasion performance of the coating films.

The organic solvent resistance rub testing reflected the chemical-resistance performance of the UV-cured coating, with ethanol and butanone being two typical solvents of concern in the 3C industry. Table 2 lists the testing results for every sample in different groups, with the number of scratches after the solvent resistance rub testing. No sample showed the phenomena of whitening and blistering, but the number of scratches increased with the loading of the bifunctional HEA-IPDI-HEA segments. Although the introduction of multi-functional modified CNTs and GO may increase the crosslinking density compared to the corresponding sample in the Ctrl group, the enhancement in the crosslinking density cannot match the density decrease caused by the increasing bifunctional HEA-IPDI-HEA segments. However, the CNT and GO themselves cannot improve the solvent-resistance property, so the results of the number of scratches increased following the loading of modified CNTs and GO in the cured coating film. Between ethanol and butanone, the coating in our system exhibited higher ethanol-resistance than did butanone. This agrees with the majority of polyurethane acrylate UV-curable coatings.

The boiling water resistance of the cured films is also shown in Table 2. It is observed that the cured films incorporated with carbon nanomaterials show an obvious improvement in boiling water resistance among the tested films. To our knowledge, the boiling water resistance mainly depends on the adhesion and the crosslinking density of the film. A good boiling water resistance can be obtained from films with good adhesion and high crosslinking density, which can be supplied by the trifunctional (HDI-HECLA)₃ and multi-functional modified carbon nanomaterials. Even an increase in the bifunctional HEA-IPDI-HEA segments decreased the crosslinking density in the Ctrl group. The introduction of a small amount of multi-functional carbon nanomaterials reversed the performance and dramatically improved the boiling water resistance of the samples in CNT and GO groups. Analogous to the RCA abrasion testing, a performance decrease was observed again in the samples that contained 1.0% CNT and GO, which was caused by the aggregation of nanomaterials and the phase separation phenomenon. In addition, it is believed that the hydrophobic property of CNTs and GO is contributory to the boiling resistance performance of our coating.

The gloss of samples containing carbon nanomaterials was lower because of the existence of the black CNTs and brown GO. The gloss suppression was increasingly heavy with increasing amounts of CNTs and GO in the film. For the Ctrl group without carbon nanomaterials, the samples kept nearly the same gloss value. The result agrees with the physical appearance shown in Figure 2. Furthermore, when the concentration of carbon nanomaterials reached 1.0%, the gloss of the corresponding samples decreased dramatically, which was also caused by the aggregation of carbon

nanomaterials.

Combining the property variations and the performance transformation, it was found that the introduction of modified CNTs and GO can improve the performance of UV-cured coatings to various degrees, depending on the exact concentration. The increased loading of these carbon nanomaterials causes a higher crosslinking density, resulting in an improved surface hardness, abrasion resistance, chemical-resistance performance and boiling water resistance. However, when too many CNTs and GO are introduced, the aggregations caused by the relatively large specific surface area of the nanomaterials have obvious effects, thus reducing these performances. Furthermore, the UV-curable coating exhibits a lower light transmissivity when more carbon nanomaterials are introduced, which influences the ultraviolet light absorbance and thus hinders the photopolymerization of the acrylates. This downgrades the performance of the UV-cured coatings. Therefore, it is very important to formulate a balanced content of carbon nanomaterials in a UV-curable coating to achieve the best performance.

4. Conclusions

With the combination of the trifunctional (HDI-HECLA)₃ with the bifunctional HEA-IPDI-HEA urethane acrylates as the reactive resin and coordinated with TMPTA as the thinner, a novel UV-curable coating matrix was designed and prepared. The obtained coating system can be cured successfully under UV radiation to achieve excellent coatings on a PC substrate with good performances. By further introducing a relatively small amount of modified CNT and GO nanomaterials into the coating system, the performances, such as thermal stability, surface hardness, adhesion, abrasive resistance, and chemical resistance, can be dramatically improved, and the composite coating can be potentially applied in the 3C industry as an excellent surface coating.

References

- [1] SpecialChem, UV Curable Resins Market to Reach USD 4.67 Billion by 2024: Grand View Research, in, <http://adhesives.specialchem.com/news/industry-news/uv-curable-market-gvr-000184138>, 2016.
- [2] R.S. Mishra, A.K. Mishra, K.V.S.N. Raju, Synthesis and property study of UV-curable hyperbranched polyurethane acrylate/ZnO hybrid coatings, *European Polymer Journal*, 45 (2009) 960-966.
- [3] J. Seo, E.-S. Jang, J.-H. Song, S. Choi, S.B. Khan, H. Han, Preparation and properties of poly(urethane acrylate) films for ultraviolet-curable coatings, *Journal of Applied Polymer Science*, 118 (2010) 2454-2460.
- [4] Z. Jiao, X. Wang, Q. Yang, C. Wang, Modification and characterization of urethane acrylate oligomers used for UV-curable coatings, *Polymer Bulletin*, 74 (2016) 2497-2511.

Table 2. Performances of UV-cured coatings on polycarbonate sheets

Sample codes	Pencil Hardness Class	Crosscut Adhesion Class	RCA Abrasion (counts) ^a	Ethanol Resistance Rub (counts) ^b	Butanone Resistance Rub (counts) ^b	Boiling Resistance ^c	Gloss (°)
0.2ctrl	1B	5B	320	4	5	5B/2.5h; 4B/3h	91.0
0.4ctrl	1B	5B	350	6	7	5B/2h; 3B/2.5h	91.9
0.6ctrl	HB	5B	390	7	10	5B/2h; 2B/2.5h	91.6
0.8ctrl	HB	5B	410	8	>10	5B/1.5h; 4B/2h	91.2
1.0ctrl	HB	5B	450	>10	>10	5B/1.5; 3B/2h	92.0
0.2GO	HB	5B	470	2	3	5B/2.5h; 4B/3h	89.3
0.4GO	HB	5B	530	1	4	5B/4h; 3B/4.5h	88.2
0.6GO	HB	5B	560	3	7	5B/5h	87.4
0.8GO	F	5B	570	3	7	5B/5h	81.3
1.0GO	F	5B	460	3	6	5B/4h; 4B/4.5h	67.3
0.2CNT	HB	5B	490	1	3	5B/2.5h; 4B/3h	89.0
0.4CNT	HB	5B	520	1	4	5B/4h; 4B/4.5h	87.6
0.6CNT	HB	5B	550	2	5	5B/5h	87.2
0.8CNT	F	5B	600	5	9	5B/5h	84.0
1.0CNT	F	5B	440	2	7	5B/4h; 2B/4.5h	61.0

a. Recorded as the number of rubs when the coating wears out.

b. None of samples presented the phenomena of whitening and blistering. The number is the count of scratches after the solvent resistance rub testing.

c. The results recorded as the crosscut adhesion class after been boiled for few hours. For example, 5B/2.5h represents that the coating's crosscut adhesion class is 5B after boiling for 2.5 h.